

UCLA

UCLA Previously Published Works

Title

Comparison of PSMA-TO-1 and PSMA-617 labeled with gallium-68, lutetium-177 and actinium-225

Permalink

<https://escholarship.org/uc/item/3608q84b>

Journal

EJNMMI Research, 12(1)

ISSN

2191-219X

Authors

Meyer, Catherine

Prasad, Vikas

Stuparu, Andreea

et al.

Publication Date

2022

DOI

10.1186/s13550-022-00935-6


Peer reviewed

ORIGINAL RESEARCH

Open Access



Comparison of PSMA-TO-1 and PSMA-617 labeled with gallium-68, lutetium-177 and actinium-225

Catherine Meyer^{1†}, Vikas Prasad^{2†}, Andreea Stuparu³, Peter Kletting², Gerhard Glatting², Jonathan Miksch², Christoph Solbach², Katharina Lueckerath^{1,4}, Lea Nyiranshuti¹, Shaojun Zhu¹, Johannes Czernin¹, Ambros J. Beer², Roger Slavik¹, Jeremie Calais¹ and Magnus Dahlbom^{1*} 

Abstract

Background: PSMA-TO-1 ("Tumor-Optimized-1") is a novel PSMA ligand with longer circulation time than PSMA-617. We compared the biodistribution in subcutaneous tumor-bearing mice of PSMA-TO-1, PSMA-617 and PSMA-11 when labeled with ⁶⁸Ga and ¹⁷⁷Lu, and the survival after treatment with ²²⁵Ac-PSMA-TO-1/-617 in a murine model of disseminated prostate cancer. We also report dosimetry data of ¹⁷⁷Lu-PSMA-TO1/-617 in prostate cancer patients.

Methods: First, PET images of ⁶⁸Ga-PSMA-TO-1/-617/-11 were acquired on consecutive days in three mice bearing subcutaneous C4-2 xenografts. Second, 50 subcutaneous tumor-bearing mice received either 30 MBq of ¹⁷⁷Lu-PSMA-617 or ¹⁷⁷Lu-PSMA-TO-1 and were sacrificed at 1, 4, 24, 48 and 168 h for ex vivo gamma counting and biodistribution. Third, mice bearing disseminated lesions via intracardiac inoculation were treated with either 40 kBq of ²²⁵Ac-PSMA-617, ²²⁵Ac-PSMA-TO-1, or remained untreated and followed for survival. Additionally, 3 metastatic castration-resistant prostate cancer patients received 500 MBq of ¹⁷⁷Lu-PSMA-TO-1 under compassionate use for dosimetry purposes. Planar images with an additional SPECT/CT acquisition were acquired for dosimetry calculations.

Results: Tumor uptake measured by PET imaging of ⁶⁸Ga-labeled agents in mice was highest using PSMA-617, followed by PSMA-TO-1 and PSMA-11. ¹⁷⁷Lu-PSMA tumor uptake measured by ex vivo gamma counting at subsequent time points tended to be greater for PSMA-TO-1 up to 1 week following treatment ($p > 0.13$ at all time points). This was, however, accompanied by increased kidney uptake and a 26-fold higher kidney dose of PSMA-TO-1 compared with PSMA-617 in mice. Mice treated with a single-cycle ²²⁵Ac-PSMA-TO-1 survived longer than those treated with ²²⁵Ac-PSMA-617 and untreated mice, respectively (17.8, 14.5 and 7.7 weeks, respectively; $p < 0.0001$). Kidney, salivary gland, bone marrow and mean \pm SD tumor dose coefficients (Gy/GBq) for ¹⁷⁷Lu-PSMA-TO-1 in patients #01/#02/#03 were 2.5/2.4/3.0, 1.0/2.5/2.3, 0.14/0.11/0.10 and $0.42 \pm 0.03/4.45 \pm 0.07/1.8 \pm 0.57$, respectively.

Conclusions: PSMA-TO-1 tumor uptake tended to be greater than that of PSMA-617 in both preclinical and clinical settings. Mice treated with ²²⁵Ac-PSMA-TO-1 conferred a significant survival benefit compared to ²²⁵Ac-PSMA-617 despite the accompanying increased kidney uptake. In humans, PSMA-TO-1 dosimetry estimates suggest increased

[†]Catherine Meyer, Vikas Prasad are Co-first authors

*Correspondence: mdahlbom@mednet.ucla.edu

¹ Ahmanson Translational Theranostics Division, Department of Molecular and Medical Pharmacology, David Geffen School of Medicine, UCLA, 650 Charles E Young Drive South, Los Angeles, CA 90095-7370, USA
Full list of author information is available at the end of the article

tumor absorbed doses; however, the kidneys, salivary glands and bone marrow are also exposed to higher radiation doses. Thus, additional preclinical studies are needed before further clinical use.

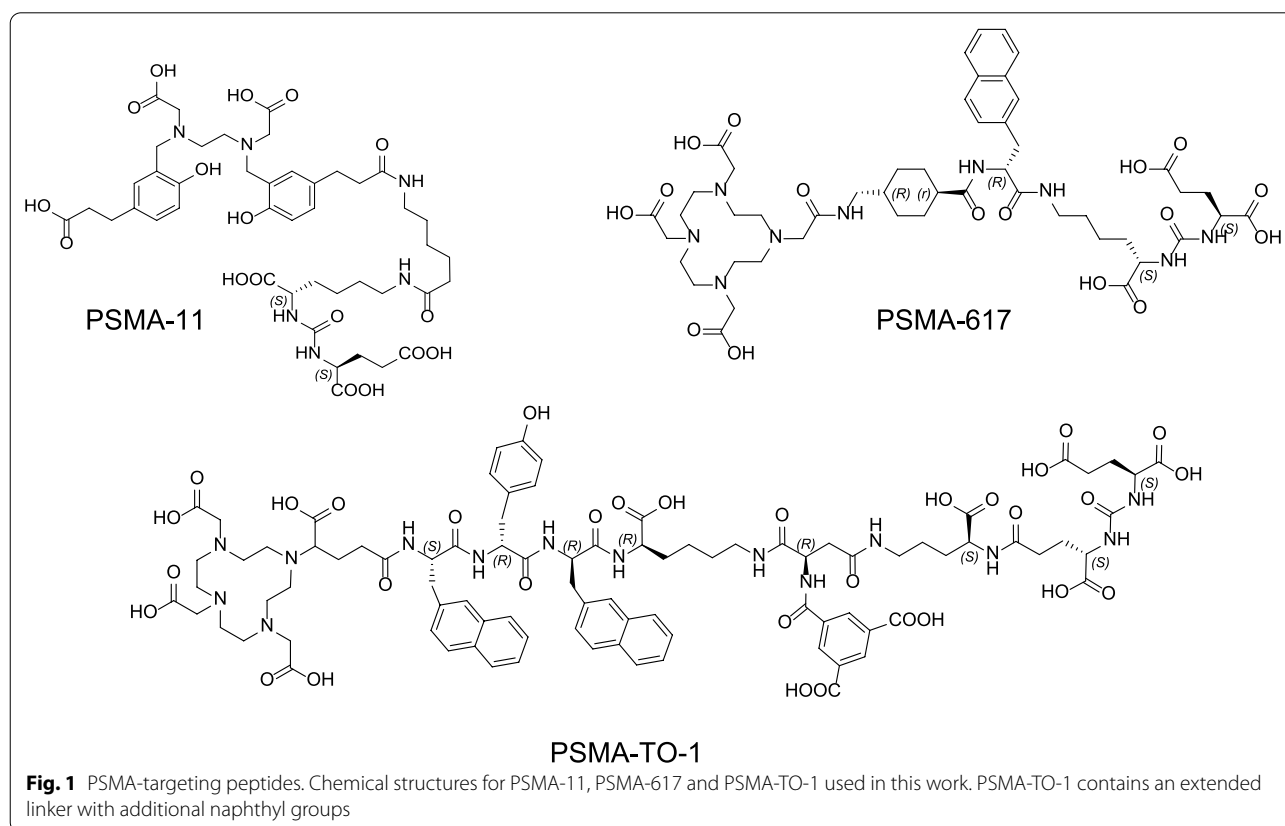
Keywords: PSMA-TO-1, PSMA-617, Prostate cancer, Radioligand therapy, Dosimetry

Introduction

The prostate-specific membrane antigen (PSMA) is highly expressed by prostate cancer (PCa) cells and is a relevant target for PCa imaging and therapy. Radioligand therapy (RLT) using PSMA-targeting ligands is an emerging therapeutic option in men with metastatic castration-resistant prostate cancer (mCRPC). However, more than half of mCRPC patients treated with PSMA RLT eventually fail therapy [1, 2]. Reasons for disease progression or patient relapse may include insufficient radiation dose delivery (due to low PSMA expression, insufficient administered activity and insufficient tumor retention time of the RLT agent) or radio resistance (tumor biology, germline or somatic mutations, DNA damage repair mechanisms) [3–8]. One potential strategy to increase tumor radiation doses is to extend the PSMA ligand circulation time. Reducing the blood clearance (by the kidneys and other off-target organs) can potentially lead to an increased tumor accumulation of

the radiolabeled peptide. One approach using an Evans blue albumin-binding moiety was shown to yield a two-fold–sixfold increase in the number of disintegrations in tumors using ^{177}Lu -EB-PSMA-617 compared to ^{177}Lu -PSMA-617 [9]. This Evans blue modification approach has also been investigated for peptide receptor radionuclide therapy which was shown to increase tumor dose relative to ^{177}Lu -DOTATATE; and, in a subsequent phase I clinical trial, improved response rates (NCT03478358) [10, 11].

In this study, we investigated a novel PSMA ligand called PSMA-TO-1 (“Tumor-Optimized-1”) that was developed for prolonged circulation time and higher tumor uptake (Dr. H.-J. Wester, Technische Universität München, Germany). In comparison with PSMA-617 and PSMA-I&T, PSMA-TO-1 contains an extended linker with additional naphthyl groups to increase albumin and other protein bindings in blood, thereby increasing the lipophilicity (chemical structures shown



in Fig. 1). Experimentally, PSMA-TO-1, also known as PSMA-71, was shown to improve internalization and exhibit greater albumin binding than both PSMA-617 and PSMA-I&T (98 vs. 74 and 78%, respectively) [12]. Additionally, in mice bearing LNCaP tumors, biodistribution data of ^{177}Lu -PSMA-TO-1 revealed threefold greater tumor uptake 24 h post-injection compared with ^{177}Lu -PSMA-I&T (14.3 ± 0.9 vs. $4.1 \pm 1.1\%$ IA/g) with an improved tumor-to-kidney uptake ratio (0.4 vs. 0.1, respectively) [12]. These promising findings warranted further exploration into the performance and application of PSMA-TO-1.

Here we directly compared preclinically PSMA-TO-1 as an imaging and therapeutic agent with the two most widely studied PSMA ligands: PSMA-11 and PSMA-617. First, we determined the biodistribution of the diagnostic compounds ^{68}Ga -PSMA-TO-1/-617/-11 in murine models. Second, we assessed *ex vivo* the biodistribution of the therapeutic compounds ^{177}Lu -PSMA-TO-1 and ^{177}Lu -PSMA-617 in a subcutaneous xenograft model. Third, we conducted a murine survival study in a model of disseminated prostate cancer to compare the therapeutic efficacy of ^{225}Ac -PSMA-TO-1 and ^{225}Ac -PSMA-617. Additionally, we report the dosimetry data of ^{177}Lu -PSMA-TO-1 in humans.

Methods

Study design

This work was investigator-initiated and self-funded. Pre-clinical experiments were conducted at UCLA (USA). Clinical procedures were performed at Ulm University (Germany). Preclinical and clinical procedures were conducted independently and separately. The clinical and preclinical studies were not planned as a translational study and were merged retrospectively into a single report.

Preclinical experiments

Cell culture

The human-derived, PSMA-expressing, castration-resistant prostate cancer tumor cell line C4-2 was used for all preclinical work (courtesy Dr. G. Thalmann; Department of Urology, Inselspital Bern, Switzerland). Cells were maintained in Roswell Park Memorial Institute 1640 medium supplemented with 10% fetal bovine serum (Omega Scientific) at 37 °C and 5% CO_2 . They were monitored regularly for mycoplasma contamination using the Venor GeM Mycoplasma Detection Kit (Sigma-Aldrich) and authenticated by short tandem repeat sequencing (August 2019; Laragen). The parental cells were engineered to express firefly luciferase (C4-2-luc) by transduction with an amphotropic retrovirus encoding

enhanced firefly luciferase followed by fluorescence-activated cell sorting of transduced cells.

Animal studies

Immunodeficient, 6–8-weeks-old NOD SCID gamma (NSG) male mice (Charles River Labs, Wilmington, MA) were housed under pathogen-free conditions with food and water *ad libitum*, and a 12–12 h light–dark cycle. Veterinarian staff and investigators observed the mice daily to ensure animal welfare and determine if humane endpoints (e.g., hunched and ruffled appearance, apathy, ulceration, severe weight loss and tumor burden) were reached. All animal studies were approved by the UCLA Animal Research Committee (# 2005–090).

Radiopharmaceutical synthesis

PSMA-11 and PSMA-617 precursors were obtained from ABX advanced biochemical compounds (Radeberg, Germany). PSMA-TO-1 precursor was obtained from Dr. H.-J. Wester (Technische Universität München, Germany). Gallium-68 was eluted from an Eckert & Ziegler IGG100 Generator and the peptide precursors (5 nmol for PSMA-11 and PSMA-TO-1; 10 nmol for PSMA-617) were labeled with ^{68}Ga to obtain 19–24 mCi of final products according to previously published protocols [13].

No-carrier-added $^{177}\text{LuCl}_3$ was obtained from Spec-tron MRC and PSMA-617 and PSMA-TO-1 were radiolabeled as previously described with a molar activity of 84 GBq/ μmol [14]. Actinium-225 was supplied by the Isotope Program within the Office of Nuclear Physics in the Department of Energy's Office of Science and radiolabeled as previously described (molar activity of 130 MBq/ μmol) [13].

^{68}Ga -PSMA-TO-1/-617/-11 PET/CT imaging in mice

NSG mice bearing subcutaneous C4-2 tumors underwent PET/CT imaging with each of the following compounds on consecutive days: ^{68}Ga -PSMA-11, ^{68}Ga -PSMA-617, and ^{68}Ga -PSMA-TO-1 in the same 3 mice. Average tumor volumes over the 3 days were 660 ± 35 mm^3 , 190 ± 32 mm^3 and 243 ± 1.5 mm^3 for mouse 1, 2 and 3, respectively. PET images were acquired 60 min after intravenous administration of 1.1 MBq ^{68}Ga -PSMA in 100 μL volume (PSMA-TO-1 on day 1; PSMA-11 on day 2; PSMA-617 on day 3) using the preclinical Genesis 8 PET/CT scanner (Sofie Biosciences). Attenuation-corrected images were reconstructed using maximum likelihood expectation–maximization with 60 iterations. The following parameters were applied for CT imaging: 40 kVp, 190 mA, 720 projections, and 55-ms exposure time per projection. The resulting PET/CT images were analyzed for tumor volume and percent injected activity uptake per gram using VivoQuant Imaging Software

(Invivo, Boston, MA). One-way ANOVA with Bonferroni's multiple comparisons test was used to compare the tumor uptake of each ligand.

¹⁷⁷Lu-PSMA-TO-1/617 *ex vivo* biodistribution study in mice

NSG mice were subcutaneously inoculated into the right shoulder region with 5 million C4-2 cells in 100 μ l matrigel ($n=50$ mice). After 3 weeks, when the average tumor size was approximately 300 mm³, mice were randomized based on tumor volume and treated with either 30 MBq of ¹⁷⁷Lu-PSMA-617 or ¹⁷⁷Lu-PSMA-TO-1 ($n=25$ mice PSMA-617; $n=25$ mice PSMA-TO-1). Treatment activity (30 MBq) was selected based on previous studies [14]. Following treatment, mice were sacrificed at 5 time points ($n=5$ mice/time point): 1, 4, 24, 48 and 168 h (7 days). The following organs were collected and weighed prior to gamma counting for activity quantification with ¹⁷⁷Lu detection energy window of 189–231 keV (Cobra II Auto-Gamma; Packard Instrument Co.): blood, tumor, submandibular salivary glands, heart, lungs, liver, bilateral kidneys, spleen, stomach (with contents), intestines (with contents), prostate, testes, muscle, femur (with and without bone marrow), bone marrow and the brain. Kidney organ doses were estimated from the measured uptake values using the 25 g mouse model in OLINDA/EXM version 2.2.0 [15]. The kidney activity data were fit and integrated to yield residence times and kidney self-doses. The multiple t test method was used for biodistribution statistical comparisons and the Holm–Sidak method was applied to determine statistical significance (set to ≤ 0.05).

²²⁵Ac-PSMA-TO-1/617 survival study in mice

NSG mice underwent intracardiac inoculation with 500,000 C4-2-luc cells (in 50 μ l PBS) to achieve widespread microscopic visceral and bone metastases, as previously described ($n=25$ mice) [13]. After 5 weeks, mice were randomized into 3 groups: treatment with ²²⁵Ac-PSMA-617 ($n=10$), treatment with ²²⁵Ac-PSMA-TO-1 ($n=10$), or untreated controls ($n=5$). Before treatment, the whole body tumor burden was assessed by bioluminescence imaging (IVIS Lumina III *in vivo* imaging system, Perkin Elmer). Treatment groups comprised equal proportions of mice with higher and lower tumor burden to create groups with comparable average tumor burden (Additional file 1: Figure S1). Two days prior to treatment, the mean bioluminescence radiance for non-treated, ²²⁵Ac-PSMA-617-, and ²²⁵Ac-PSMA-TO-1-treated mice was $2.23 \times 10^9 \pm 1.46 \times 10^9$ p/sec/cm²/sr ($n=5$), $2.07 \times 10^9 \pm 2.09 \times 10^9$ ($n=10$), and $2.37 \times 10^9 \pm 1.56 \times 10^9$ ($n=10$), respectively (not significantly different; $p > 0.42$ for all group comparisons). The treatment activity was selected as 40 kBq ²²⁵Ac for both

the PSMA-TO-1 and 617 groups based on previous studies [16]. Mice were sacrificed when they exhibited severe weight loss and showed signs of deteriorating health such as hunching, dehydration, and labored breathing. The overall condition of the animals was assessed using the body conditioning score [17]. A drop in score from 3 (well-conditioned mouse) to 2 (under-conditioned; segmentation of vertebral column evident, dorsal pelvic bones palpable) warranted euthanasia. The Log-rank (Mantel–Cox) statistical test was used for survival analysis (GraphPad Prism 8).

Clinical procedures

Patients

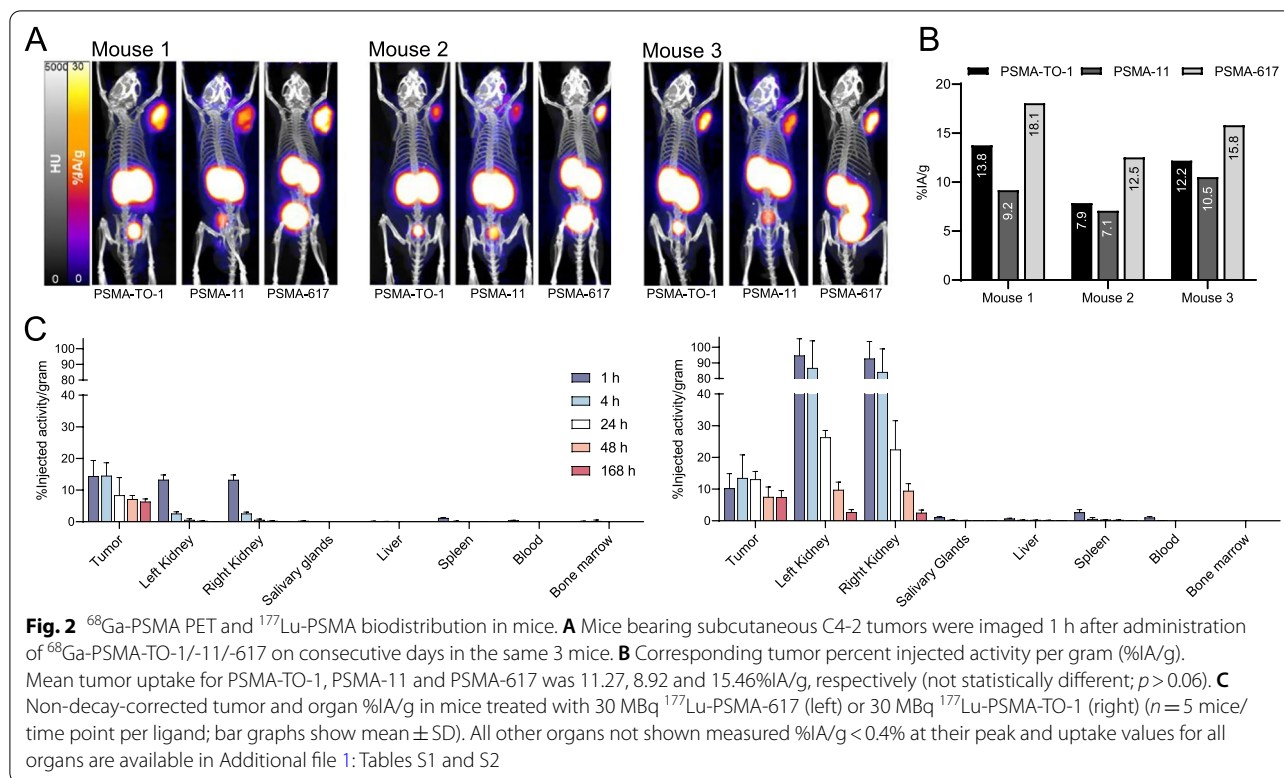
This was a retrospective evaluation of three patients with mCRPC. All patients had end-stage progressive mCRPC disease after all conventional therapies had failed and were referred by their treating uro-oncologist for ¹⁷⁷Lu-PSMA therapy under compassionate use in compliance with the German Medicinal Products Act, AMG §13 (2b). All three patients gave written informed consent to undergo ⁶⁸Ga-PSMA PET/CT scans and potential ¹⁷⁷Lu-PSMA-TO-1 therapy after multiple time point dosimetry imaging following national regulations, the updated Declaration of Helsinki, and Good Clinical Practice (GCP). The radiopharmaceuticals were produced in accordance with the German Medicinal Products Act §13(2b) and the responsible regulatory bodies.

Radiosynthesis of ⁶⁸Ga-PSMA-11 and ⁶⁸Ga-PSMA-TO-1 for clinical application

PSMA-11 precursor was obtained from ABX advanced biochemical compounds (Radeberg, Germany). PSMA-TO-1 precursor was obtained from Dr. H.-J. Wester (Technische Universität München, Germany). For the production of ⁶⁸Ga-radiopharmaceuticals for clinical use, a 50 mCi iThemba ⁶⁸Ge/⁶⁸Ga-generator (iThemba LABS, South Africa) was used. ⁶⁸Ga-PSMA-11 and ⁶⁸Ga-PSMA-TO-1 were synthesized in a fully automated (Scintomics Gallelut radiosynthesizer) and GMP-compliant process adapted from the data presented previously by Eder et al. [18] by use of 20 μ g PSMA-11 precursor (⁶⁸Ga-PSMA-11) and 80 μ g PSMA-TO-1 precursor (⁶⁸Ga-PSMA-TO-1), respectively.

¹⁷⁷Lu-PSMA-TO-1 human dosimetry

Lutetium-177 was acquired from ITM (Garching, Germany) and radiolabeling was performed according to the established procedure in a GMP-certified radiopharmacy laboratory. All three patients were injected with 500 MBq of ¹⁷⁷Lu-PSMA-TO-1; a sub-therapeutic activity for dosimetry calculation purposes. Planar images were acquired at 1–2 h, 3–4 h, 18–24 h,



42–48 h and 90–164 h with an additional SPECT/CT image acquisition at 18–24 h. The first image was used to determine the 2D calibration factor; planar images from 3 to 48 h aided in identifying the peak in tumor tissue uptake; finally, planar images from 90 to 164 h were used to measure late-phase kinetics. Blood samples were drawn at regular intervals: 10 min, 1 h, 4 h, 24 h and 48 h. Time–activity data were derived from the images and blood samples using NUKDOS software [19]. The image acquisition was performed on a Siemens Symbia T2 SPECT/CT scanner equipped with medium energy parallel-hole collimators. Measurements were done with an energy window between 190 and 225 keV. SPECT was acquired with 30 projections per head on a body contour trajectory with a 128×128 matrix and a 30 s acquisition duration per projection. Attenuation correction was based on a low-dose CT scan. SPECT was reconstructed iteratively using the ordered subsets expectation maximization algorithm with 8 iterations, 15 subsets, and a post-reconstruction Gaussian filtering with a filter size of 12 mm. All corrections were executed according to MIRD Pamphlets No. 16 and 26 [20, 21]. For each patient, the kidney with the highest uptake and two tumor lesions were segmented manually. The quantification for the SPECT/CT system was performed using phantom-derived calibration factors with a NEMA phantom that yielded a camera

sensitivity of 678 cpm/MBq. The pharmacokinetic information was obtained from the 2D images. For each data set, an exponential fit function was selected based on visual inspection, the standard error, the correlation matrix, and the Akaike information criterion (AIC) [19]. The settings for the measurement error were model-based and a fractional measurement error of 10% was assumed for blood, total body, and kidney, and 15% for tumors [19].

Dosimetry of ¹⁷⁷Lu-PSMA-617 was also performed 7 days after the ¹⁷⁷Lu-PSMA-TO-1 administration in one patient (patient #03), using 500 MBq of ¹⁷⁷Lu-PSMA-617 and a similar method as outlined above. Images were acquired at 1 h, 4 h, 24 h and 48 h, with blood samples taken at 10 min, 1 h, 4 h, 24 h and 48 h, taking into account the remaining activity of ¹⁷⁷Lu-PSMA-TO-1. The latest imaging time point was set to 48 h since the late-phase kinetics for PSMA-617 are known, and to reduce patient burden. No subsequent therapy with ¹⁷⁷Lu-PSMA-TO-1 was performed.

⁶⁸Ga-PSMA-TO-1 human PET/CT human images

⁶⁸Ga-PSMA-TO-1 PET/CT was performed in one patient (patient #01). ⁶⁸Ga-PSMA-TO-1 PET/CT images were acquired at 60 min and 120 min after injection of 180 MBq of ⁶⁸Ga-PSMA-TO-1.

Results

Preclinical studies

⁶⁸Ga-PSMA-TO-1/-617/-11 preclinical PET/CT imaging

All ⁶⁸Ga-labeled PSMA-TO-1, PSMA-11, and PSMA-617 PET images showed high tumor accumulation 1 h after tail vein injection (Fig. 2A). Tracer clearance was predominantly via urinary excretion. We observed the greatest tumor uptake (%IA/g) for PSMA-617, followed by PSMA-TO-1 and PSMA-11 in all three mice (Fig. 2B). Mean tumor uptake for PSMA-TO-1, PSMA-11 and PSMA-617 was 11.27, 8.92 and 15.46%IA/g, respectively. The difference in mean tumor uptake between ligands was not statistically significant ($p > 0.06$ for all group comparisons).

¹⁷⁷Lu-PSMA-TO-1/-617 ex vivo biodistribution study

Ex vivo counts of ¹⁷⁷Lu-PSMA-617 and ¹⁷⁷Lu-PSMA-TO-1 revealed predominant uptake in the subcutaneous tumors and kidneys (Fig. 2C). Consistent with the ⁶⁸Ga-PSMA-TO-1/-617 PET imaging findings, tumor uptake at 1 h post-administration tended to be higher for ¹⁷⁷Lu-PSMA-617 than ¹⁷⁷Lu-PSMA-TO-1, though it did not reach statistical significance (14.4 vs. 10.2%IA/g; $p = 0.207$). At all subsequent measurement time points, the absolute tumor uptake tended to be higher for PSMA-TO-1 than PSMA-617 ($p > 0.13$ for all time points). However, kidney uptake was also higher (24%IA/g 24 h after administration, compared with 0.54%IA/g using PSMA-617; $p = 0.0001$, $n = 5$ mice [10 kidneys] per time point per compound). Kidney residence times for ¹⁷⁷Lu-PSMA-617 and ¹⁷⁷Lu-PSMA-TO-1 were 2.00E-01 and 5.34E00 MBq-h/MBq, respectively. This translates to a 26 times greater effective dose in the kidneys for PSMA-TO-1 compared with PSMA-617 (5.41E01 vs. 1.44E03 mSv/MBq; or, 43 Sv vs. 1.6 Sv for an injected activity of 30 MBq).

²²⁵Ac-PSMA-TO-1/-617 survival study

²²⁵Ac-PSMA-617 and ²²⁵Ac-PSMA-TO-1 both significantly prolonged median overall survival relative to untreated mice (7.7 vs. 14.5 and 7.7 vs. 17.8 weeks; $p < 0.0001$). The survival benefit conferred by mice treated with ²²⁵Ac-PSMA-TO-1 was statistically significant compared to treatment with ²²⁵Ac-PSMA-617 ($p = 0.0002$) (Fig. 3).

Patients

The clinical characteristics of the three patients are summarized in Table 1. Of note, patient #01 had multiple liver metastases with low PSMA-expression. Patient #02 had diffuse bone involvement and could not complete the ¹⁷⁷Lu-PSMA-617 image acquisitions (and therefore

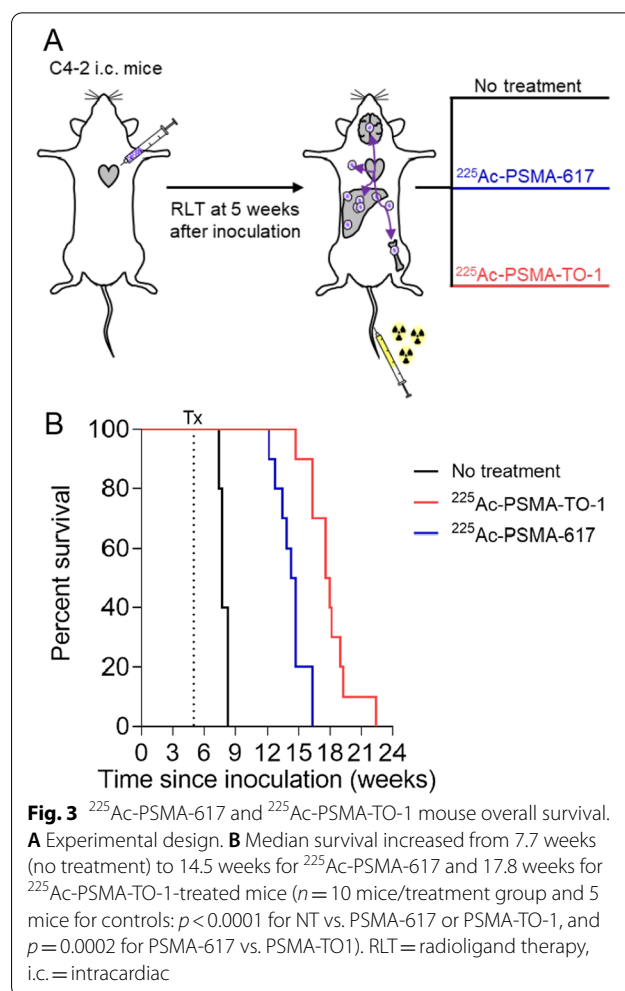


Fig. 3 ²²⁵Ac-PSMA-617 and ²²⁵Ac-PSMA-TO-1 mouse overall survival. **A** Experimental design. **B** Median survival increased from 7.7 weeks (no treatment) to 14.5 weeks for ²²⁵Ac-PSMA-617 and 17.8 weeks for ²²⁵Ac-PSMA-TO-1-treated mice ($n = 10$ mice/treatment group and 5 mice for controls; $p < 0.0001$ for NT vs. PSMA-617 or PSMA-TO-1, and $p = 0.0002$ for PSMA-617 vs. PSMA-TO-1). RLT = radioligand therapy, i.c. = intracardiac

dosimetry) because he developed acute renal failure 5 days after administration of 500 MBq of ¹⁷⁷Lu-PSMA-TO-1. This was likely due to tumor lysis syndrome (see laboratory test in Additional file 1: Figure S2). Despite receiving a sub-therapeutic administered activity, his PSA value decreased after normalization of kidney function (Additional file 1: Figure S2B) and his ECOG performance improved from 3 to 1, suggesting anti-tumor treatment effect.

¹⁷⁷Lu-PSMA-TO-1 human dosimetry

Kidney, salivary gland, bone marrow and mean \pm SD tumor dose coefficients (Gy/GBq) of ¹⁷⁷Lu-PSMA-TO-1 in patients #01, #02, #03 were 2.5/2.4/3.0, 1.0/2.5/2.3, 0.14/0.11/0.10 and $0.42 \pm 0.03/4.45 \pm 0.07/1.80 \pm 0.57$, respectively (Table 2). In patient #03, for whom a dosimetry comparison between PSMA-TO-1 and PSMA-617 could be completed, the therapeutic index (mean tumor dose/critical organ dose) of ¹⁷⁷Lu-PSMA-617/¹⁷⁷Lu-PSMA-TO-1 for the kidney, bone marrow and

Table 1 Patients' clinical characteristics

Patient #	Age (years)	PSA (ng/ml)	Prior therapy	miTNM stage
#01	58	320	Bicalutamide enzalutamide, docetaxel, cabazitaxel	T3 N1 M1c (liver)
#02	49	2914	LHRH, bicalutamide enzalutamide, docetaxel, 2 × ¹⁷⁷ Lu-PSMA 617	Tx Nx M1a M1b (bone, lymph nodes)
#03	60	100	Docetaxel, samarium, enzalutamide, 4 × ¹⁷⁷ Lu-PSMA 617	T4 N1 M1a M1b (bone, lymph nodes)

PSA prostate-specific antigen, LHRH luteinizing hormone-releasing hormone

Table 2 Clinical dosimetry results

Organ	¹⁷⁷ Lu-PSMA-TO-1 dose coefficients (Gy/GBq)			¹⁷⁷ Lu-PSMA-617 dose coefficients (Gy/GBq)
	Patient #01	Patient #02	Patient #03	
Kidneys	2.5	2.4	3.0	0.6
Salivary gland	1.0	2.5	2.3	1.1
Bone marrow	0.14	0.11	0.10	0.033
Tumor 1	0.40	4.4	2.2	1.10
Tumor 2	0.44	4.5	1.4	0.80

salivary gland was 1.6/0.6, 28.8/18.0 and 0.9/0.8, respectively (Fig. 4). Due to the higher uptake in critical organs, no subsequent radionuclide therapy with ¹⁷⁷Lu-PSMA-TO-1 was done.

⁶⁸Ga-PSMA-TO-1 PET/CT human images

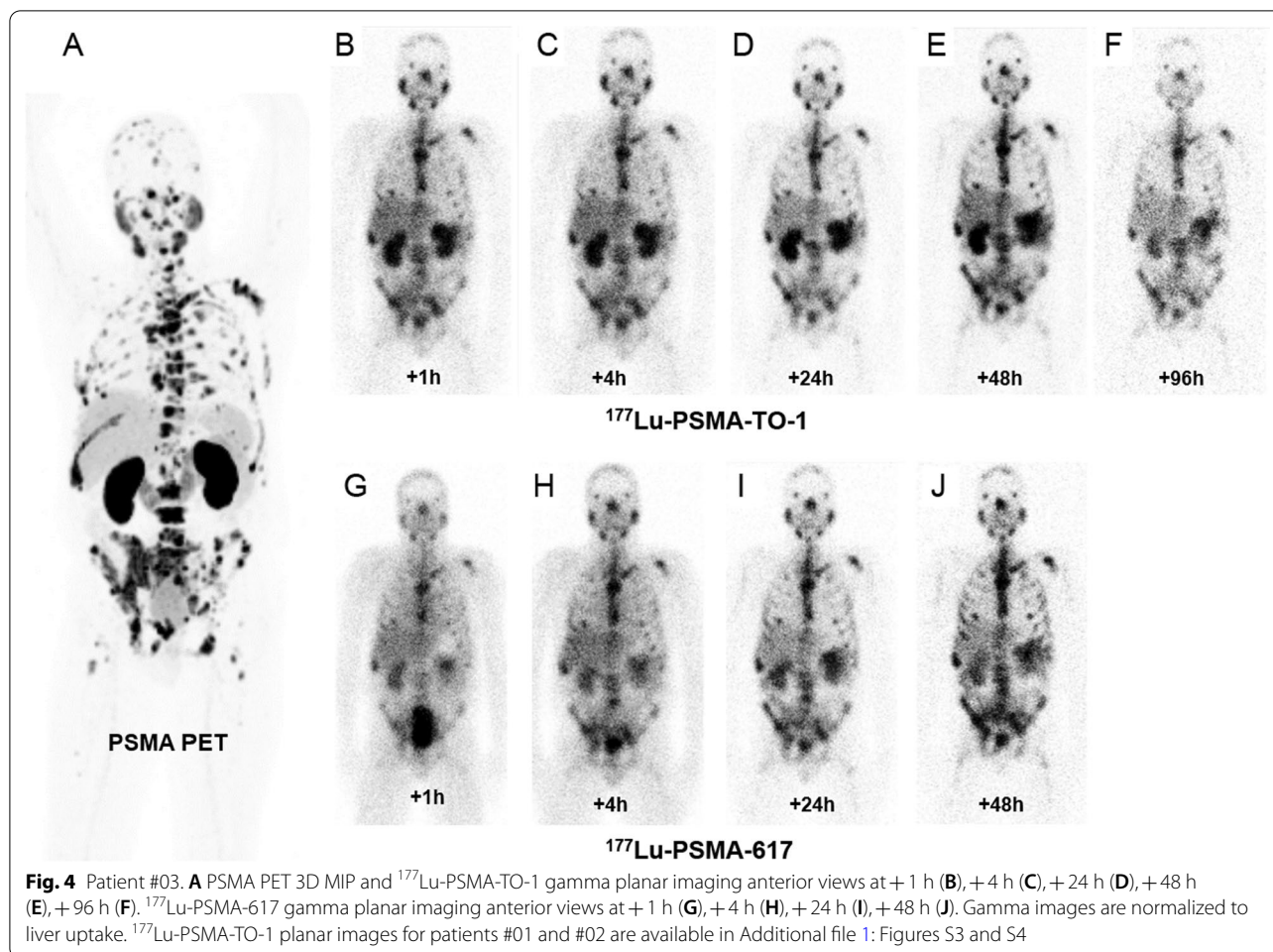
For patient #01, who underwent both ⁶⁸Ga-PSMA-TO-1 and ⁶⁸Ga-PSMA-11 PET/CT at 60 min, blood pool activity and kidney uptake were higher with PSMA-TO-1 than with PSMA-11: SUV_{mean} 4.0 vs 1.0 and 30 vs. 14, respectively. Tracer uptake in liver metastases was higher with ⁶⁸Ga-PSMA-TO-1 compared to ⁶⁸Ga-PSMA-11: SUV_{mean} 6.0 vs. 4.0. At 120 min, ⁶⁸Ga-PSMA-TO-1 uptake in metastases increased (SUV_{mean} 8.0, +33%), whereas blood pool uptake remained constant (see Fig. 5 and Table 3).

Discussion

In this work, we first examined preclinically the biodistribution of 3 PSMA-targeting compounds in tumor-bearing mice. The tumor uptake was higher with PSMA-TO-1 than with PSMA-617 at all measured time points after 1 h. Most notably, this increased tumor uptake was accompanied by murine kidney uptake that was 44 times higher with PSMA-TO-1 than with PSMA-617 24 h after administration, which translates to a 26-fold greater kidney dose in mice. Nevertheless, the preclinical survival

study indicated that mice treated with ²²⁵Ac-PSMA-TO-1 conferred a significant survival benefit compared to those treated with ²²⁵Ac-PSMA-617 (median overall survival 17.8 vs. 14.5 weeks; $p=0.0002$). However, long-term nephrotoxic effects could not be studied as the time for histologically measurable parenchymal damage can be greater than 6 months in murine models [22, 23] and euthanasia was required within 7–18 weeks of treatment in all mice.

In humans, we observed the kidney dose coefficients to be 6–8 times higher with ¹⁷⁷Lu-PSMA-TO-1 than with ¹⁷⁷Lu-PSMA-617 (2.4–3.0 Gy/GBq in this study vs. 0.39 Gy/GBq for PSMA-617, as published elsewhere [4]). It should be noted that these estimates reflect PSMA-TO-1 doses from 3 patients only, thereby limiting the broad translatability of these results. The kidneys are a primary dose-limiting organ in PSMA-targeted RLT, with commonly used maximum tolerated dose thresholds ranging from 18 to 28 Gy (derived from external beam RT studies) [20, 24]. However, the low dose rate radiation delivered by RLT differs from the high dose rate of external beam RT, and biologically effective doses up to 40 Gy with low dose rate RLT may be well-tolerated [20]. This may in part be explained by the relatively short survival of patients who may not live to experience renal toxicity. Future work may include preclinical approaches to quantify acute kidney damage with molecular or pathological



biomarkers as predictors for long-term injury. One study by Pellegrini et al. identified γ -H2AX positive nuclei in the renal cortex, a marker for DNA strand breaks, as a possible indicator for long-term radiation-induced kidney damage [23]. However, meaningful translations of preclinical observations related to renal damage are confounded by the relatively increased radio resistance of murine kidneys compared to humans [25, 26]. Further preclinical studies will be required to better assess the potential nephrotoxic risk of ^{177}Lu -PSMA-TO-1 before further clinical use.

We observed reversible renal insufficiency in patient #02, which may be explained by tumor lysis syndrome rather than toxicity. Patient #02 had diffuse bone marrow involvement and developed suspected tumor lysis syndrome one week after receiving only 500 MBq of ^{177}Lu -PSMA-TO-1, and 2 weeks after 500 MBq of ^{177}Lu -PSMA-617. Tumor lysis syndrome was supported by the subsequent drop in serum PSA levels and normalization of kidney function. This suggests the delivery of high radiation to bone metastases even from a

sub-therapeutic administered activity of 500 MBq of ^{177}Lu -PSMA-TO-1. However, higher tumor doses may present a potential for treating a patient population with bone or bone marrow lesions. Since PSMA-TO-1 is a longer-circulating peptide, higher bone marrow doses were expected. Indeed, dosimetry data of Patient #03 revealed a threefold higher bone marrow dose with PSMA-TO-1 compared to PSMA-617 (Table 2). Comparing our bone marrow dose in three patients with a larger PSMA-617 cohort [27], the bone marrow dose is 8–tenfold higher for PSMA-TO-1 than with PSMA-617. While this higher dose could pose more risk for hematotoxicity, greater bone marrow exposure and thereby dose delivery may be efficacious to treat patients with bone marrow involvement. At the same time, it should also be considered in the setting of severe bone marrow infiltration whether treatment with a beta- or alpha-emitting radionuclide may be more appropriate. It has been postulated that the shorter tissue penetration range of alpha-emitters, such as ^{225}Ac , may be favored in settings where the need to spare surrounding tissue

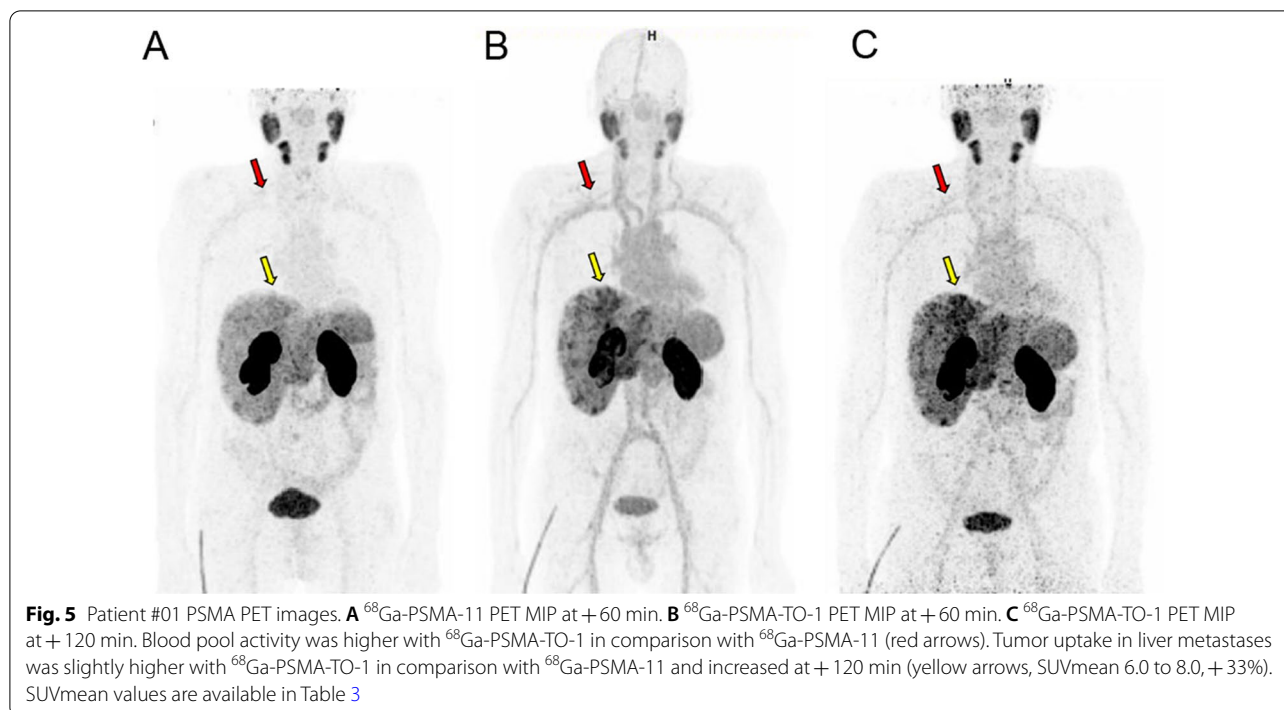


Table 3 ⁶⁸Ga-PSMA-TO-1 and ⁶⁸Ga-PSMA-11 PET/CT SUVs in patient #01

Organ	SUVmean		
	⁶⁸ Ga-PSMA-TO-1 60 min	⁶⁸ Ga-PSMA-11 60 min	⁶⁸ Ga-PSMA-TO-1 120 min
Blood pool	4	1	4
Spleen	6	6	6
Kidneys	30	14	24
Salivary glands	6	9	10
Liver metastasis	6	4	8

SUV standardized uptake value

is of greater concern, such as to minimize bone marrow toxicity [28–30].

Finally, another organ of interest in PSMA-targeted RLT is the salivary gland. In this study, the dose coefficient to the salivary glands was two times greater for PSMA-TO-1 compared with PSMA-617 (2.3 vs. 1.1 Gy/GBq in the same patient). The current literature reports salivary gland dose coefficients from ¹⁷⁷Lu-PSMA-617 treatment ranging from 0.44 and 0.58 Gy/GBq [4] (for submandibular and parotid glands, respectively) to 1.4 Gy/GBq [27]. While xerostomia resulting from ¹⁷⁷Lu-PSMA RLT is not as frequent nor severe as observed in ²²⁵Ac-PSMA RLT, the possible clinical significance of increased salivary gland uptake in ¹⁷⁷Lu-PSMA RLT remains to be characterized. Overall, the

higher uptake in normal organs in both preclinical and clinical settings necessitates further preclinical testing and optimization before further clinical use.

Conclusion

Tumor uptake tended to be greater with PSMA-TO-1 than with PSMA-617 in both preclinical and early clinical settings. Preclinical studies demonstrated a significant survival benefit with ²²⁵Ac-PSMA-TO-1 over ²²⁵Ac-PSMA-617. However, a dosimetry comparison of ¹⁷⁷Lu-PSMA-TO-1 and ¹⁷⁷Lu-PSMA-617 in one patient suggested that PSMA-TO-1 exposes the kidneys, salivary glands and bone marrow to higher radiation absorbed doses. Before further clinical use, preclinical optimization is required.

Abbreviations

AIC: Akaike information criterion; ANOVA: Analysis of variance; CT: Computed tomography; DNA: Deoxyribonucleic acid; ECOG: Eastern Cooperative Oncology Group; IA/g: Injected activity per gram; mCRPC: Metastatic castration-resistant prostate cancer; MIRD: Medical internal radiation dose; NSG: NOD SCID gamma; PET: Positron emission tomography; PSA: Prostate-specific antigen; PSMA: Prostate-specific membrane antigen; RLT: Radioligand therapy; SD: Standard deviation; SPECT: Single-photon emission computed tomography.

Supplementary Information

The online version contains supplementary material available at <https://doi.org/10.1186/s13550-022-00935-6>.

Additional file 1: Supplementary preclinical and clinical information.

Acknowledgements

Not applicable.

Author contributions

RS, VP, AB, JCz, AS, MD, CM, JCa and SZ contributed to conception and design. CM, VP, AS, KL, LN, JM and CS acquired the data. CM, VP, PK, GG, JM, CS and JCa analyzed and interpreted the data. CM, VP, JCa, MD, PK, JCz and AB contributed to writing and/or revision of the manuscript. Dr. P. Kletting, who made significant intellectual contributions to the work, has since passed away during final preparations of the manuscript. All other authors read and approved the final manuscript.

Funding

JCz is the recipient of a grant from the Prostate Cancer Foundation (19CHAL09) and the Jonsson Comprehensive Cancer Center NIH-NCI Cancer Center Support Grant (P30 CA016042). JCa is the recipient of grants from the Prostate Cancer Foundation (20YOUN05), the Society of Nuclear Medicine and Molecular imaging (2019 Molecular Imaging Research Grant for Junior Academic Faculty), the Philippe Foundation Inc. (NY, USA) and the ARC Foundation (France) (SAE20160604150). The funding bodies did not participate in the design of the study and collection, analysis and interpretation of data and in writing the manuscript.

Availability of data and materials

All preclinical data analyzed during this study are included in this published article and in supplementary materials. Additional clinical data are available from the authors upon reasonable request.

Declarations**Ethics approval and consent to participate**

All animal studies were approved by the UCLA Animal Research Committee (# 2005–090) and carried out in compliance with the ARRIVE guidelines for reporting of research involving animals. All patients were referred for ¹⁷⁷Lu-PSMA therapy under compassionate use in compliance with the German Medicinal Products Act, AMG §13 (2b). All three patients gave written informed consent to undergo ⁶⁸Ga-PSMA PET/CT scans and potential ¹⁷⁷Lu-PSMA-TO-1 therapy following national regulations, the updated Declaration of Helsinki, and Good Clinical Practice.

Consent for publications

Not applicable.

Competing interests

The authors have declared that no competing interests relevant to this article exist. KL reports paid consulting activities for Sofie Biosciences/iTheranostics, and funding from AMGEN outside of the submitted work. JC is a cofounder of and holds equity in Sofie Biosciences and Trethera Therapeutics. JCa reports prior consulting activities for Advanced Accelerator Applications, Blue Earth Diagnostics, Curium Pharma, GE Healthcare, EXINI, IBA RadioPharma, Janssen Pharmaceuticals, Lantheus, POINT Biopharma, Progenics, Radiomedix, and Telix Pharmaceuticals.

Author details

¹Ahmanson Translational Theranostics Division, Department of Molecular and Medical Pharmacology, David Geffen School of Medicine, UCLA, 650 Charles E Young Drive South, Los Angeles, CA 90095-7370, USA. ²Department of Nuclear Medicine, University Hospital Ulm, Ulm, Germany. ³Atreca, Inc., South San Francisco, CA, USA. ⁴Clinic for Nuclear Medicine, University Hospital Essen, Essen, Germany.

Received: 6 June 2022 Accepted: 16 September 2022

Published online: 01 October 2022

References

1. Heck MM, Tauber R, Schwaiger S, Retz M, D'Alessandria C, Maurer T, et al. Treatment outcome, toxicity, and predictive factors for radioligand

- therapy with (177)Lu-PSMA-I&T in metastatic castration-resistant prostate cancer. *Eur Urol*. 2019;75(6):920–6.
2. Violet J, Sandhu S, Irvani A, Ferdinandus J, Thang S-P, Kong G, et al. Long-term follow-up and outcomes of retreatment in an expanded 50-patient single-center phase II prospective trial of ¹⁷⁷Lu-PSMA-617 theranostics in metastatic castration-resistant prostate cancer. *J Nucl Med*. 2020;61(6):857–65.
3. Chan TG, O'Neill E, Habjan C, Cornelissen B. Combination strategies to improve targeted radionuclide therapy. *J Nucl Med*. 2020;61(11):1544–52.
4. Violet J, Jackson P, Ferdinandus J, Sandhu S, Akhurst T, Irvani A, et al. Dosimetry of (177)Lu-PSMA-617 in metastatic castration-resistant prostate cancer: correlations between pretherapeutic imaging and whole-body tumor dosimetry with treatment outcomes. *J Nucl Med Off Publ Soc Nucl Med*. 2019;60(4):517–23.
5. Scott A, Bodei L. Pharmacogenomics in radionuclide therapy: impact on response to theranostics. *J Nucl Med*. 2020. <https://doi.org/10.2967/jnumed.120.254995>.
6. Czernin J, Current K, Mona CE, Nyiranshuti L, Hikmat F, Radu CG, et al. Immune-checkpoint blockade enhances (225)Ac-PSMA617 efficacy in a mouse model of prostate cancer. *J Nucl Med Off Publ Soc Nucl Med*. 2021;62(2):228–31.
7. Current K, Meyer C, Magyar CE, Mona CE, Almajano J, Slavik R, et al. Investigating PSMA-targeted radioligand therapy efficacy as a function of cellular PSMA levels and intratumoral PSMA heterogeneity. *Clin Cancer Res Off J Am Assoc Cancer Res*. 2020;26(12):2946–55.
8. Stuparu AD, Capri JR, Meyer C, Le TM, Evans-Axelsson SL, Current K, et al. Mechanisms of resistance to prostate-specific membrane antigen-targeted radioligand therapy in a mouse model of prostate cancer. *J Nucl Med Off Publ Soc Nucl Med*. 2020. <https://doi.org/10.2967/jnumed.120.256263>.
9. Zang J, Fan X, Wang H, Liu Q, Wang J, Li H, et al. First-in-human study of ¹⁷⁷Lu-EB-PSMA-617 in patients with metastatic castration-resistant prostate cancer. *Eur J Nucl Med Mol Imaging*. 2019;46(1):148–58.
10. Liu Q, Zang J, Sui H, Ren J, Guo H, Wang H, et al. Peptide receptor radionuclide therapy of late-stage neuroendocrine tumor patients with multiple cycles of (177)Lu-DOTA-EB-TATE. *J Nucl Med Off Publ Soc Nucl Med*. 2021;62(3):386–92.
11. Zhang J, Wang H, Jacobson O, Cheng Y, Niu G, Li F, et al. Safety, pharmacokinetics, and dosimetry of a long-acting radiolabeled somatostatin analog (177)Lu-DOTA-EB-TATE in patients with advanced metastatic neuroendocrine tumors. *J Nucl Med Off Publ Soc Nucl Med*. 2018;59(11):1699–705.
12. Wester H-J, inventorPSMA ligands for imaging and endoradiotherapy2020.
13. Stuparu AD, Meyer CAL, Evans-Axelsson SL, Lückerrath K, Wei LH, Kim W, et al. Targeted alpha therapy in a systemic mouse model of prostate cancer—a feasibility study. *Theranostics*. 2020;10(6):2612–20.
14. Fendler WP, Stuparu AD, Evans-Axelsson S, Luckerath K, Wei L, Kim W, et al. Establishing (177)Lu-PSMA-617 radioligand therapy in a syngeneic model of murine prostate cancer. *J Nucl Med Off Publ Soc Nucl Med*. 2017;58(11):1786–92.
15. Stabin MG, Sparks RB, Crowe E. OLINDA/EXM: the second-generation personal computer software for internal dose assessment in nuclear medicine. *J Nucl Med Off Publ Soc Nucl Med*. 2005;46(6):1023–7.
16. Miederer M, Scheinberg DA, McDevitt MR. Realizing the potential of the actinium-225 radionuclide generator in targeted alpha particle therapy applications. *Adv Drug Deliv Rev*. 2008;60(12):1371–82.
17. Ullman-Culleré MH, Foltz CJ. Body condition scoring: a rapid and accurate method for assessing health status in mice. *Lab Anim Sci*. 1999;49(3):319–23.
18. Eder M, Schäfer M, Bauder-Wüst U, Hull W-E, Wängler C, Mier W, et al. ⁶⁸Ga-complex lipophilicity and the targeting property of a urea-based PSMA inhibitor for PET imaging. *Bioconjug Chem*. 2012;23(4):688–97.
19. Kletting P, Schimmel S, Hanscheid H, Luster M, Fernandez M, Nosske D, et al. The NUKDOS software for treatment planning in molecular radiotherapy. *Z Med Phys*. 2015;25(3):264–74.
20. Ljungberg M, Celler A, Konijnenberg MW, Eckerman KF, Dewaraja YK, Sjogreen-Gleisner K, et al. MIRD pamphlet No. 26: joint EANM/ MIRD guidelines for quantitative ¹⁷⁷Lu SPECT applied for dosimetry of radiopharmaceutical therapy. *J Nucl Med Off Publ Soc Nucl Med*. 2016;57(1):151–62.

21. Siegel JA, Thomas SR, Stubbs JB, Stabin MG, Hays MT, Koral KF, et al. MIRD pamphlet no. 16: techniques for quantitative radiopharmaceutical bio-distribution data acquisition and analysis for use in human radiation dose estimates. *J Nucl Med Off Publ Soc Nucl Med*. 1999;40(2):375–61s.
22. Cohen EP, Robbins ME. Radiation nephropathy. *Semin Nephrol*. 2003;23(5):486–99.
23. Pellegrini G, Siwowska K, Haller S, Antoine DJ, Schibli R, Kipar A, et al. A short-term biological indicator for long-term kidney damage after radionuclide therapy in mice. *Pharmaceuticals (Basel)*. 2017. <https://doi.org/10.3390/ph10020057>.
24. Emami B, Lyman J, Brown A, Coia L, Goitein M, Munzenrider JE, et al. Tolerance of normal tissue to therapeutic irradiation. *Int J Radiat Oncol Biol Phys*. 1991;21(1):109–22.
25. Augustine AD, Gondré-Lewis T, McBride W, Miller L, Pellmar TC, Rockwell S. Animal models for radiation injury, protection and therapy. *Radiat Res*. 2005;164(1):100–9.
26. Schüler E, Larsson M, Parris TZ, Johansson ME, Helou K, Forssell-Aronsson E. Potential biomarkers for radiation-induced renal toxicity following 177Lu-octreotate administration in mice. *PLoS ONE*. 2015;10(8):e0136204.
27. Delker A, Fendler WP, Kratochwil C, Brunegrab A, Gosewisch A, Gildehaus FJ, et al. Dosimetry for (177)Lu-DKFZ-PSMA-617: a new radiopharmaceutical for the treatment of metastatic prostate cancer. *Eur J Nucl Med Mol Imaging*. 2016;43(1):42–51.
28. Haberkorn U, Giesel F, Morgenstern A, Kratochwil C. The future of radioligand therapy: α , β , or both? *J Nucl Med*. 2017;58(7):1017–8.
29. Kojima S, Cuttler JM, Shimura N, Koga H, Murata A, Kawashima A. Present and future prospects of radiation therapy using α -emitting nuclides. *Dose Response A Publ Int Hormesis Soc*. 2018;16(1):1559325817747387.
30. Morgenstern A, Apostolidis C, Kratochwil C, Sathekge M, Krolicki L, Bruchertseifer F. An overview of targeted alpha therapy with (225)actinium and (213)bismuth. *Curr Radiopharm*. 2018;11(3):200–8.

Publisher's Note

Springer Nature remains neutral with regard to jurisdictional claims in published maps and institutional affiliations.

Submit your manuscript to a SpringerOpen[®] journal and benefit from:

- Convenient online submission
- Rigorous peer review
- Open access: articles freely available online
- High visibility within the field
- Retaining the copyright to your article

Submit your next manuscript at ► [springeropen.com](https://www.springeropen.com)
